Robotica (2024), **42**, pp. 3731–3747
doi:10.1017/S0263574724001619

CAMBRIDGE UNIVERSITY PRESS

RESEARCH ARTICLE

A novel mobile robot with origami wheels designed for navigating sandy terrains

Junfeng Hu, Shen Shu and Weitao Han

School of Mechanical and Electrical Engineering, Jiangxi University of Science and Technology, Ganzhou, China
Corresponding author: Junfeng Hu; Email: hjfsuper@126.com

Received: 13 January 2024; **Revised:** 19 May 2024; **Accepted:** 17 June 2024; **First published online:** 21 October 2024

Keywords: origami mobile robot; sandy terrains; Kresling origami; slipping ratio; origami wheel

Abstract

Sand robots play a vital role as mobile tools for human exploration of desert regions, facilitating resource transportation and exploration. However, desert areas primarily consist of beaches or dunes, resulting in a highly diverse and complex terrain environment that demands enhanced adaptability from sandy mobile robots. Traditional wheeled robots currently face challenges such as skidding, limited climbing ability, and inadequate obstacle avoidance capabilities in sandy environments. To address these issues and enable effective adaptation to the intricate sand environment, we propose a novel sandy mobile robot equipped with Kresling origami wheels. The origami wheel can dynamically adjust its width and morphology through Kresling origami folding. Experimental tests were conducted to illustrate the impact of width variation on the robot's mobility velocity, propulsive force, climbing performance, and carrying capacity. The self-folding malleability of the origami wheel empowers the robot to efficiently accomplish diverse tasks, including swift movement on flat sand surfaces, seamless crossing of narrow channels, and intelligent obstacle avoidance. By successfully completing these multimodal tasks while adapting to varying requirements, our robot demonstrates promising prospects for practical applications of mobile robots equipped with origami wheels – paving the way for wider adaptation and utilization of sand mobile robots.

1. Introduction

The utilization of robots in sandy terrains has been primarily focused on their ability to navigate and operate effectively in desert environments, making them highly desirable for a wide range of applications such as desert exploration, agriculture, mining, and rescue operations [1–5]. Moreover, the potential application of sand robots extends to lunar exploration due to the similarity between the moon's surface covered in fine dust known as regolith and sandy terrains [6–8]. However, designing versatile and adaptable sandy robots that meet specific application requirements poses a significant challenge.

It is challenging for rigid robots to navigate on sandy terrain, even for nimble robots that struggle with the loose sand [9–11]. In comparison to agile creatures, most robots have limited adaptability and mobility on complex sandy surfaces. Enhancing the locomotive performance of robotic systems in such environments requires improved structural design. This is because sand can exhibit both liquid-like and solid-like behavior, which depends on its interaction with the robotic systems [8]. Conventional robots often become trapped in loose sand due to their weight and lack the necessary propulsive force to overcome obstacles like bunkers. As a result, these robots are unable to adapt to changes in the sandy environment and gradually sink deeper into sand pits. Although researchers have extensively studied wheeled locomotion on sand, it remains a challenge for wheeled robots to dynamically adjust the size and shape of their wheels.

The locomotion of wheeled vehicles on flowing sand differs from that on hard ground due to the combined solid- and fluid-like forces experienced by the wheels during surface penetration.

Traversing varying sand terrains poses challenges for planetary rovers and earthbound rescue robots, making it difficult to design a robot capable of handling such conditions [6]. A solution proposed was a sand robot with six C-shaped legs, utilizing their agility to navigate through sand [9]. However, rapid movement of the limbs could cause deep sinking into the sand, while the rigidity of its legs prevents adaptation to complex sandy terrains. To address this issue, a control system equipped with sensors can be constructed to provide feedback on the robot's situation and adjust its locomotion accordingly to meet the demands of sandy environments. Nevertheless, integration requirements for such a control system make this solution complicated. An alternative approach involves designing reconfigurable wheels that can change their shape and configuration to adapt to changing sandy terrains.

Most of the robots designed for operation in sandy environments are wheeled mobile robots. To address the limitations of these robots in such conditions, specialized wheels are employed to enhance their performance. By increasing the contact area with sand, the interaction force between the wheel and sand is amplified. This can be achieved through two approaches: incorporating spiked designs into the wheels and widening their dimensions. The design principle behind these sand wheels aims to augment adaptability in sandy environments by maximizing tire surface–sand contact. In soft sand terrains, wheeled mobile robots often encounter issues like slipping and sinking, which impede normal locomotion, particularly when traversing sand dunes. To effectively operate in the complex sandy environment, locomotion patterns observed in animal species serve as a valuable source of inspiration for designing sand robots. Drawing inspiration from the versatile movements exhibited by desert spiders, a spider-inspired sandy robot equipped with a double-six-bar-closed-chain 5R mechanism. This innovative design enables the robot to perform handsprings, crawling, and cartwheel motions.

The weight of the robot causes the soft sand to collapse beneath the wheels, forming a small sandpit, and due to inadequate traction from loose sand interacting with the wheels, crossing the sandpit becomes challenging. The rapidly rotating wheels sink deeper into the sandpit, eventually rendering passage impossible. To address this issue, wheeled mobile robots can enhance their performance in sandy environments by modifying wheel design. Several studies have focused on increasing the contact area between wheeled wheels and sand through tread optimization, thereby improving obstacle-crossing capabilities in soft sandy soil conditions. For instance, equidistant metal plates are added to the wheel's tread surface and auxiliary wheel claws are installed.

The art of origami, renowned for its intricate paper folding techniques, has emerged as a valuable source of inspiration for designing robotic structures owing to its capacity to generate complex shapes and versatile patterns through folding creases [12–15]. By integrating origami-inspired folding mechanisms, sand robots can significantly augment their mobility and adaptability in sandy environments. For instance, the application of origami structures in constructing the robot's wheels enables them to dynamically alter their shape and size, facilitating navigation across diverse terrains such as rocky surfaces or sandy dunes.

The mobility of wheeled robots in unstructured sandy terrain is severely constrained by the heterogeneous properties of granular media, including particle size and shape, friction, and compaction [16–18]. To enhance their locomotion capabilities, one promising approach involves the utilization of deformable wheels. By incorporating a variable-diameter wheel design inspired by origami-based soft robotics principles, the robot can effectively traverse not only high obstacles but also narrow gaps [19–23].

The challenge of enabling wheeled robots to traverse sandy terrain lies in the design of a reconfigurable wheel capable of effectively navigating such environments. Our study investigates the utilization of origami wheels to facilitate the optimal operation of our robot on sand. Sections 2 and 3 delineate the design aspects and key features of our sand robot. Finally, we present conclusions and discuss the significance of our innovative sandy robot.

https://doi.org/10.1017/S0263574724001619 Published online by Cambridge University Press

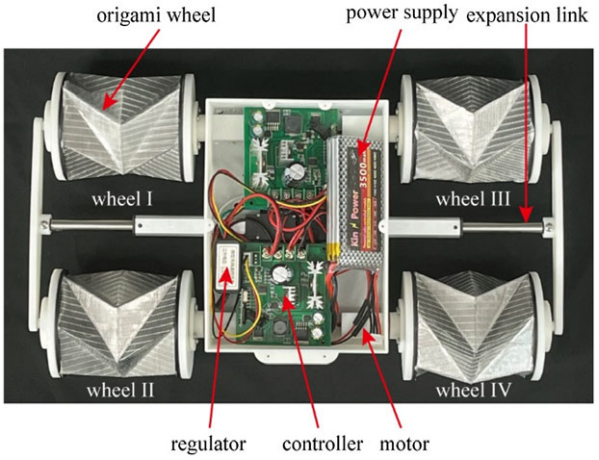

Figure 1. *Sand robot.*

2. Design of origami sand robot

The sand robot consists of four origami wheels, a robot body, an expansion link, and a control system (refer to Fig. 1). The origami wheel incorporates a Kresling origami mechanism in its design. The robot body is constructed as a rectangular box with dimensions of 180 mm length, 130 mm width, and 80 mm height. To minimize weight, the body is fabricated using polylactic acid. The control system comprises two motors, a regulator, and a power supply. Each pair of front origami wheels (wheel I and II) as well as rear wheels (wheel III and IV) are individually controlled by dedicated motors connected through couplings. By employing speed controllers that regulate rotation via pulse-width modulation signals, precise manipulation of the rotational speed of the wheels can be achieved. To ensure uninterrupted mobility on sandy terrains while maintaining compactness, the control system is enclosed within the robot body. For extended operation time without compromising safety or performance, a polymer rechargeable lithium battery with stable endurance and high energy safety capabilities serves as the power supply for the sand robot. This battery provides an output voltage of 12 V along with a power capacity of 3500 mAh. These specifications guarantee prolonged movement capability for the sand robot even under demanding conditions. Due to their lightweight of the origami materials, the combined weight of all components amounts to only 1.12 kg.

The wheel demonstrates exceptional stiffness to effectively adapt to the challenging sandy environment. We employ a rigid material, namely pure titanium sheet with a thickness of 0.2 mm, for constructing the origami wheel. However, this choice presents challenges in achieving the desired configuration through folding techniques. The fabrication process of the origami wheel is depicted in Fig. 2. It encompasses four distinct steps: (I) a laser cutting machine (Model LM-3030 from Jinan Leman numerical control equipment Co., LTD) is utilized to precisely cut a specific number of triangular sheets from a larger piece of titanium sheeting. (II) These individual titanium metal sheets are then meticulously positioned on mesh fiber tape with high viscosity following the Kresling crease pattern guidelines. (III) To ensure optimal alignment and cohesion between adjacent triangular titanium sheets, an additional layer of mesh fiber tape is applied on the opposite side of the Kresling origami plate as well. (IV) Finally, any excess fiber tape along the perimeter is carefully trimmed and folded along creases to construct a double-layer symmetrical Kresling origami structure.

The working principle of the sand-moving robot is depicted in Fig. 3. The motor generates torque T_t, which acts upon the origami wheel. Under the influence of this torque, the wheel exerts a rim force F_o on the sand. In accordance with Newton's third law, the reaction force F_t exerted by the sand on the origami wheel serves as the propulsive force driving forward motion of the robot. When there is sufficient adhesion between the origami wheel and the sand, that is, when slippage does not occur, the reaction

https://doi.org/10.1017/S0263574724001619 Published online by Cambridge University Press

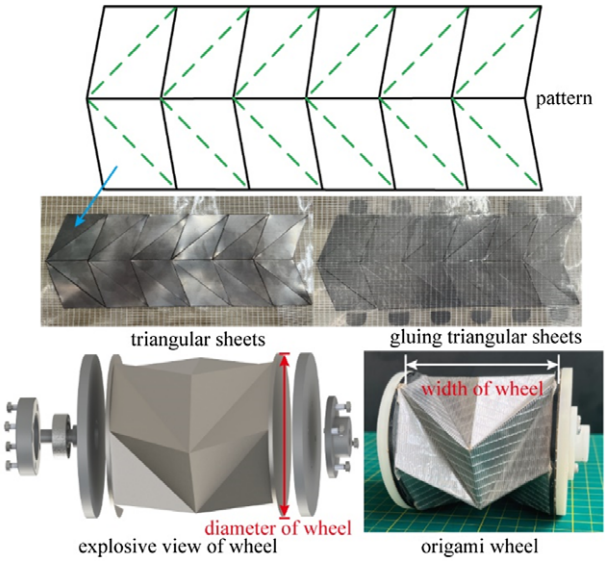

Figure 2. *Fabrication of origami wheel.*

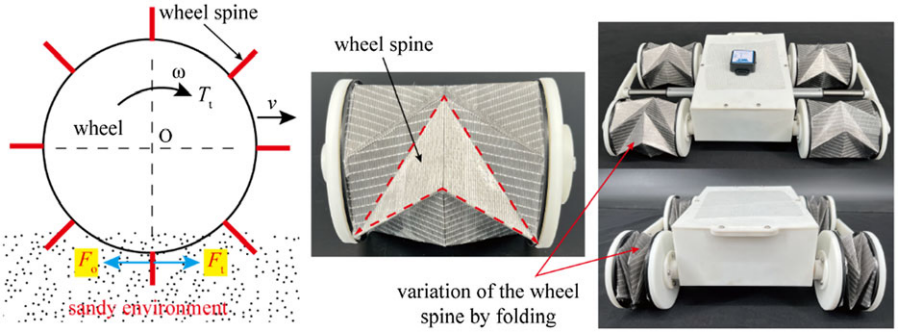

Figure 3. *Working principle of the sand robot.*

force from the sand acts upon the origami wheel along its circumference, thereby propelling the robot forward on sandy terrain. The folding surface of the origami structure and the concave surface formed by the creases are equivalent to some wheel spines like tire patterns of the car wheel. By manipulating folding and unfolding of the origami wheel, the wheel spine pattern, depth, and contact area with sand will vary. These variations can influence the propelling force and the friction effect between the wheel and sandy environment.

The Kresling origami structure is equipped with two thin round plates (2 mm thickness) made of acrylic, which have the same diameter as the origami itself. These plates are securely affixed at both ends of the origami to ensure its structural stability. To enhance support in sandy environments, we have devised inner and outer circular wheel plates that are firmly attached to both ends of the origami mechanism using adhesive bonding. Moreover, a coupling bolted to the inner wheel plate is employed for connecting the origami wheel with the body of the sand robot.

To enhance the adaptability of the robot in sandy terrains, we employ the folding mechanism of origami wheels to adjust their width. A telescopic rod equipped with a built-in linear motor is utilized for expanding or contracting the origami wheels through pushing and pulling actions. Two external connecting rods are attached to the left and right wheels, respectively. The telescopic rod drives these connecting rods, enabling contraction or expansion of the origami structure and thus adjusting the

https://doi.org/10.1017/S0263574724001619 Published online by Cambridge University Press

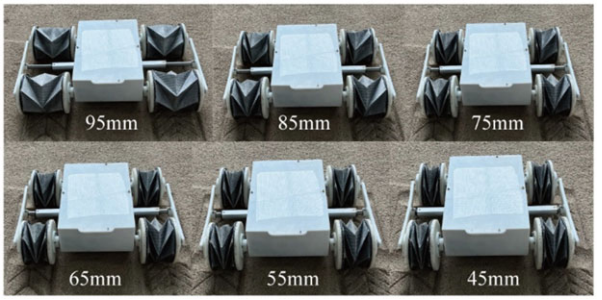

Figure 4. *Width variation of the origami wheel.*

wheel width accordingly. Telescopic rod I controls the width of the left wheels, while telescopic rod II adjusts the width of the right wheels. Both telescopic rods are precisely regulated for accurate control. Figure 4 illustrates how manipulation of these telescopic rods leads to variations in wheel width. Under thrust from an electrically powered telescopic rod, maximum wheel width can reach 95 mm, while minimum wheel width is set at 45 mm. This allows for a range in wheel widths from 45 to 95 mm, achieving an impressive ratio between maximum and minimum widths up to 19/9 (approximately 2:1). Such flexibility in wheel adjustment enables effective adaptation of our robot across diverse sandy environments.

3. Performances of the sand robot

To showcase the versatility of the sand robot equipped with an origami wheel, we conducted a series of experiments to accentuate its inherent advantages.

3.1. Locomotion capabilities

The motion performance of the robot pertains to its ability to navigate in a straight line within a sandy environment. To assess the robot's motion speed, we employed a high-speed camera manufactured by Aoni Corp. to capture the robot's movement at a frame rate of 30 frames per second. To determine the velocity of the robot, we measured the time (t) it took for the robot to travel a specific distance (d). Hence, the velocity of the robot can be calculated as the ratio between distance and time (Fig. 5a).

The motion characteristics of our sandy robot were showcased through construction and analysis within a controlled flat sand environment measuring dimensions of length (2.6 m), width (1.2 m), and thickness (50 mm). Initially, we investigated how variations in origami wheel speeds influenced our robot's velocity by setting rotational speeds at intervals ranging from 20 to 140 rpm (Fig. 5b). Our findings demonstrate a linear increase in velocity as rotational speed escalates; specifically, when set at its maximum value (140 rpm), our sandy robot achieved an impressive velocity reaching up to approximately 56 cm/s – indicating its remarkable capability for swift movement within sand.

To demonstrate the influence of different wheel widths on the velocities of the sandy robot, we folded origami wheels with varying widths of 45, 70, and 90 mm, respectively. The motion trajectories of robots equipped with wheels of different widths are depicted in Fig. 5(c) when the wheel rotation speed is set to 40 rpm. We utilized an attitude transducer to measure the velocities corresponding to different wheel sizes (as shown in Fig. 5c). The velocity of the robot exhibits a slight increase from 15 to 17 cm/s as the width of the wheel's increases. It can be observed that changes in width have minimal impact on the robot's velocity.

The robot traversing on a sandy environment requires a certain amount of time to transition from a stationary state to uniform motion, indicating an initial acceleration process. To demonstrate the impact

https://doi.org/10.1017/S0263574724001619 Published online by Cambridge University Press

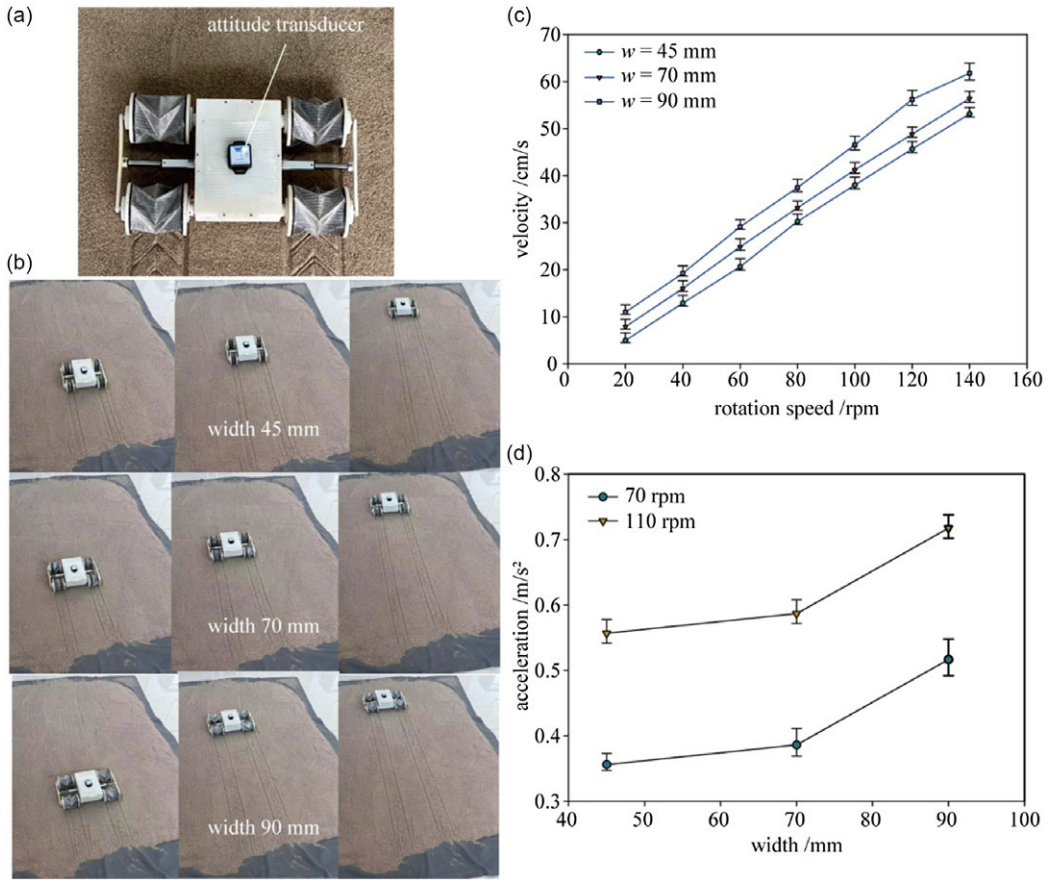

Figure 5. *Velocity analysis of the robot. (a) Experiment test setup. (b) The movement of the robot at different wheel widths. (c) Velocity variation with respect to the rotation speed and width of the wheel. (d) The acceleration of the robot with respect to the rotation speed and width of the wheels.*

of origami wheel width on this starting process, we utilize an attitude transducer for measuring the robot's acceleration. Figure 5(d) illustrates the variation in acceleration as the wheel width ranges from 45 to 90 mm. The sandy robot exhibits higher acceleration with increasing width, suggesting that wider origami wheels facilitate a shorter start-up process for the robot. Consequently, folding the origami wheels can expedite this initiation phase. The influence of wheel speed on the acceleration of the robot (Fig. 5d) was analyzed, revealing that an increase in wheel speed significantly enhanced the robot's initial acceleration and facilitated its prompt attainment of uniform motion. This improvement can be attributed to the increased propulsion force generated by higher wheel speeds.

Meanwhile, we observed that the sand robot exhibits the ability to traverse on wet sands, allowing it to effectively penetrate the substrate. The depth of wheel sinking directly influences the robot's velocity as depicted in Fig. 6. While the robot maintains a high speed across the wet sand terrain, its velocity gradually decreases with deeper penetration into the moist sand. Our experimental results validate the exceptional locomotion characteristics of our sand robot. The deceleration of the robot is attributed to wheel slippage in sandy terrain. To illustrate this phenomenon, slip resistance can be enhanced by increasing the number of concave origami surfaces resembling thorns on the wheels. To demonstrate this concept, we fabricated two origami wheels with six and eight sides, respectively, and conducted tests to analyze their motion speed under varying depths of sand. The results revealed that a higher number of

https://doi.org/10.1017/S0263574724001619 Published online by Cambridge University Press

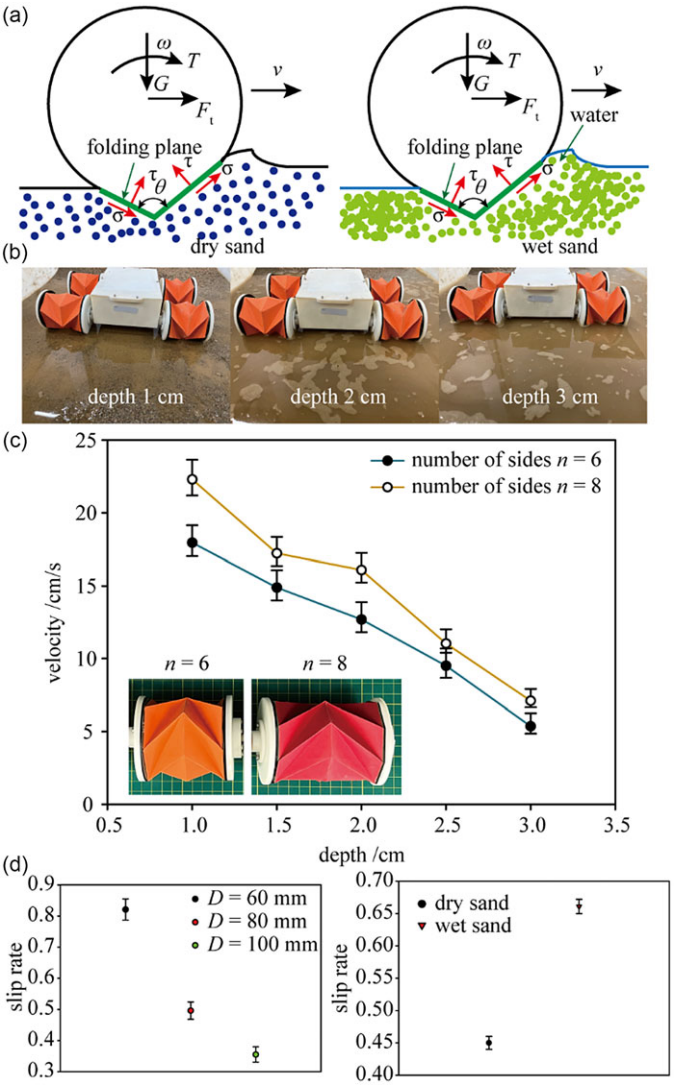

Figure 6. *Velocity profile as the wheels sink into wet sand at different depths. (a) Interactions of sand and wheels. (b) The situation of the robot sinking into wet sand. (c) The robot's velocity corresponding to varying depth and sides of origami wheel. (d) Influence of wheel diameter and sand humidity on the sliding rate of robot.*

sides on the wheel corresponded to an increased presence of thorns, resulting in reduced sliding and a slight improvement in speed.

The analysis of the disparity between wheels in dry sand and wet sand begins with an examination of the interaction between wheels and sand. This is depicted in Fig. 6(a), which illustrates their interaction. The contact region between the origami wheel and sand, as depicted in Fig. 6(a), is determined by a concave V-shaped spine formed by the folding surface. When the V-shaped spines come into contact with the sand, mutual positive pressure σ is generated between the folding surface and sand, resulting in friction (grip force) τ. This grip force prevents sliding of the wheels on the sand, and the horizontal component of this force τ propels the robot forward. Thus, driving force relies on both positive pressure between the folding surface of the origami structure and sand as well as their interfacial area for adhesion.

https://doi.org/10.1017/S0263574724001619 Published online by Cambridge University Press

These two factors can be adjusted through modifications to the origami structure's fold pattern; widening of an origami wheel increases its V-shaped concave angle θ formed by its folding surface, enlarging its contact area with sand, and enhancing resistance to sliding while providing greater propulsion force. Dry sand exhibits higher granular looseness compared to wet sand and therefore possesses a higher coefficient of friction that resists sliding motion. Conversely, water present in wet sand reduces frictional interaction between wheels and sandy surfaces, making them more prone to slide. Additionally, when encountering wet sand conditions, folded surfaces have smaller contact areas with respect to dry sands. If sliding occurs under such circumstances, grip force is lost which significantly hampers movement through sandy terrains. Consequently, robots experience reduced speed when traversing wet sands.

To enable the robot's adaptation to various types of sand, we provide the material requirements for origami wheels. The origami wheel should possess a certain level of stiffness and strength to effectively adapt to the interaction between the wheel and various types of sand, given its hardness. To prevent wheel slippage in sandy terrain, it is essential to utilize origami paper with a high coefficient of friction for its folding plate. The folding plate of the origami wheel is constructed using pure titanium material with a thickness of 0.2 mm. Furthermore, considering the folding of mountain and valley folds in the origami wheels, this specific component requires fatigue resistance and elasticity; hence high-viscosity mesh fiber tape is employed.

We conducted an analysis on the disparity in wheel diameter movement between dry sand and wet sand conditions. When traversing sandy terrain, if the external force required to propel the robot forward surpasses the maximum static friction, it becomes uncertain whether simple rolling of the origami wheel can be ensured; instead, there is a possibility of sideways sliding or even rotational motion, impeding forward progress. Folding the origami wheel leads to an increase in width which enhances friction at its interface with sand. This amplifies the "friction effect" and effectively mitigates tendencies for skidding or slipping while enhancing adaptability to sandy environments. The larger diameter of the wheel augments contact area with sand, thereby increasing friction between the wheel and sand surface, thus facilitating movement in wet sand conditions. However, this increase in wheel diameter also adds weight to the robot, making it more prone to getting stuck in dry sand. To demonstrate the contrasting sliding behavior of the wheel in dry and wet sand, we conducted an analysis on the sliding rate of the same wheel in both conditions (Fig. 6d). The results indicate that origami wheels exhibit a higher sliding rate in wet sand, suggesting their increased propensity for sliding in such environments. Furthermore, to examine the impact of wheel diameter on its sliding performance, we analyzed the sliding rate of origami wheels with diameters 60, 80, and 100 mm, respectively. It was observed that as the wheel diameter increases, there is a corresponding decrease in slip rate (Fig. 6d), implying that larger wheel diameters contribute to reducing robot slippage on sandy surfaces.

3.2. Propulsive force analysis

The propulsive force is a quantification of the sand impact on the robot. To measure this force, we utilize the push–pull dynamometer (ELK-200 produced by Elek Electric Corp.), which applies resistance to bring the robot to a stationary position while its wheels rotate at a specific speed (Fig. 7a). In this state, the dynamometer records the propelling force exerted by the robot. Notably, the rotational speed of the origami wheel directly influences this propulsive force. Figure 7(c) illustrates their linear relationship, demonstrating their proportional increase with each other. This incremental change aligns with how velocity and rotational speed interrelate in robots. Consequently, through interaction between the origami wheel and sand, propulsion is generated, enabling efficient locomotion for our sandy robot.

The width of the wheel ranges from 45 to 95 mm through the folding of the Kresling origami wheel, while maintaining a constant rotation speed. A push–pull rod is employed to investigate its impact on propulsion force. The corresponding propulsive forces for each wheel width are illustrated in Fig. 7(d). As the origami wheel expands, an increased contact area with the sand leads to an augmentation in

https://doi.org/10.1017/S0263574724001619 Published online by Cambridge University Press

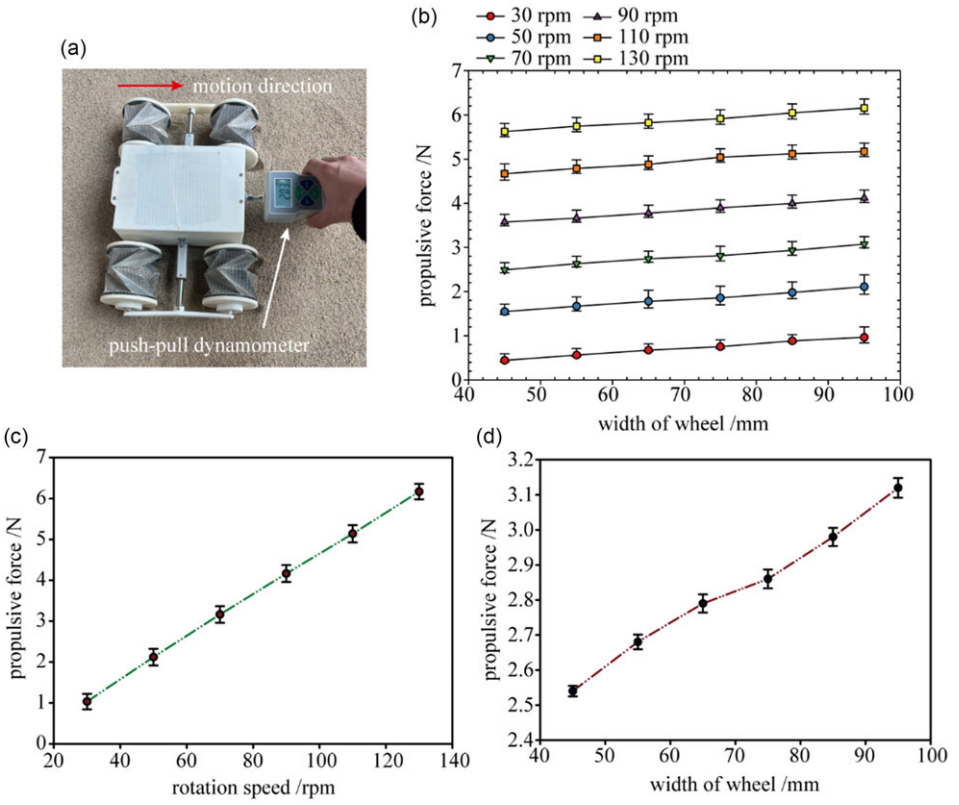

Figure 7. *Analysis of the propulsion force of the sand robot. (a) Experimental setup. (b) The propulsive force corresponding to different width and rotation speed. (c) The impact of the rotation speed on the propulsion force. (d) The influence of the width of the origami wheels on the propulsive force.*

propulsion force. The propulsive force of the robot is generated through the interaction between the wheels and the sand, ensuring a slip-free contact. This force is influenced by the contact area between the wheel and sand surface. As the wheel width increases from 45 to 65 mm, both contact area and thrust exhibit a nearly linear growth pattern. However, when the width reaches 75 mm, due to reduced depth in the concave region formed by folding surfaces and creases, there is a decrease in contact surface area. Consequently, this prevents an increase in propulsion force proportionate to its original relationship with width, thereby deviating from a linear increment. This adaptability of origami wheels enables adjustment of the wheel width in diverse sandy environments where insufficient propulsion impedes locomotion.

3.3. Steering performance of the sand robot

Steering is a crucial performance parameter for mobile robots designed for sand environments. The robot achieves straight or steering motion by adjusting the speed of its four wheels. When the left wheels (wheels I and II in Fig. 1) rotate at the same speed as the right wheels (wheel III and IV), the robot moves along a straight path. However, when there is a difference in rotational speeds between the left and right wheels, the robot exhibits steering behavior. In case of encountering an obstacle, the robot can effectively avoid it by executing turning maneuvers. Specifically, if the speed of the left wheels exceeds that of the right ones, then a right turn is executed; conversely, if the speed of left wheels is lower than that of right ones, then a left turn occurs. Figure 8(a) visually demonstrates this steering capability exhibited

https://doi.org/10.1017/S0263574724001619 Published online by Cambridge University Press

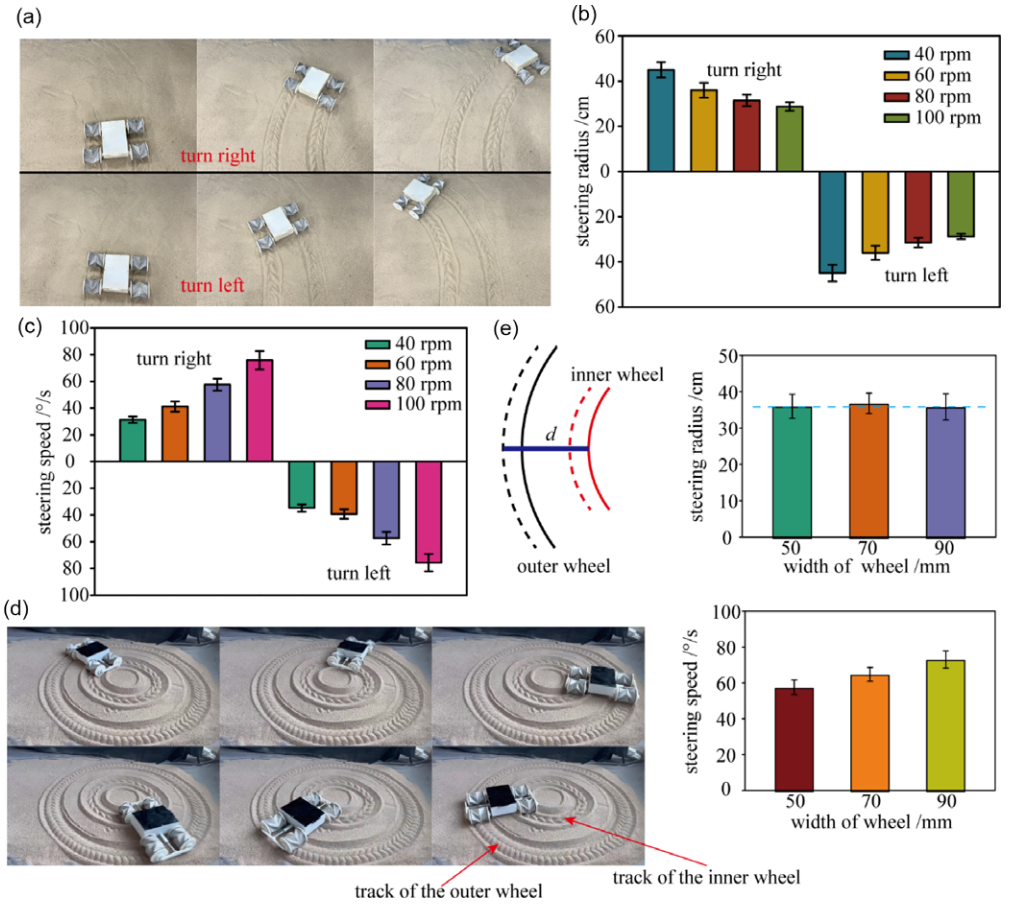

Figure 8. *Steering performance of sandy robot. (a) The snapshots reflecting the robot's steering performance. (b) The variation of steering radius with respect to the difference of the rotation speed. (c) The variation of steering speed with respect to the difference of the rotation speed. (d) Track of the outer and inner wheels (e) The steering radius with respect to the width of wheels.*

by our sandy terrain-adapted robot. To evaluate and quantify its steering characteristics accurately, we employ both steering speed and radius measurements on our sandy terrain robot platform. For measuring these parameters precisely during experiments, we utilize a gyroscope (Model: BWT61CL from Witt Intelligent Company) to capture real-time data on steering angle and angular velocity exhibited by our sandy terrain robot prototype during various maneuvers. Additionally, we determine precise values for steering radius using measurement scales based on wheel marks (as shown in Fig. 8a) imprinted on sand surfaces during different stages of maneuvering.

The turning motion of a robot involves the wheels following an arc trajectory, resulting in unequal distances traveled by the inside and outside wheels. To compensate for this discrepancy, different speeds are required, thereby utilizing the disparity between the two wheels to achieve effective turning.

The steering is determined by the speed difference between the left and right wheels. Therefore, we conducted an analysis on how this speed difference affects both the steering velocity and radius. The turning radius can be determined by calculating the speed differential between the inner and outer wheels. Its mathematical representation is as follows: $r = 2/[d * (v_o + v_o/v_i - v_i)]$, where d is the distance between the two wheels, v_o and v_i are the speed of the outer wheel and inner wheel, respectively. Specifically, we set the speed difference within a range of 40–100 rpm with intervals of 20 rpm. Figure 8(b) illustrates

https://doi.org/10.1017/S0263574724001619 Published online by Cambridge University Press

the variation in steering radius for both left and right turns as influenced by the speed difference. It can be observed that as the speed difference increases, the steering radius decreases accordingly. In other words, when navigating through wide curves, it is necessary to adjust the speed difference to a smaller value; conversely, when maneuvering tight corners, increasing the speed difference becomes essential. Interestingly though, while an increase in speed difference leads to a decrease in steering radius, it has an opposite effect on steering velocity (as depicted in Fig. 8c). Herein lies another important finding – as we increase the speed difference between wheels, we observe an increment in steering velocity. To evaluate the impact of wheel width on the steering radius, we conducted experimental analysis with varying wheel widths of 50, 70, and 90 mm. The resulting changes in steering radius are depicted in Fig. 8(e). Notably, our findings indicate that the influence of wheel width on the steering radius is negligible. To elucidate this outcome further, Fig. 8(d) illustrates the trajectories followed by both outer and inner wheels during a turn. The turning radius is determined by disparities in speed and separation between these two wheels. Importantly, when maintaining an equal difference in speed, increasing the width of both wheels (as indicated by the dotted line in Fig. 8e) does not alter their distance apart. This observation provides a plausible explanation for why wheel width has no discernible effect on the turning radius. The turning speed of the robot was also tested while varying the width of the folded wheel (Fig. 8e). The test results indicated a slight improvement in the turning speed with an increase in wheel width, as wider wheels provided greater propulsion force, aligning with the findings observed for linear motion (Fig. 5c).

3.4. Capability to traverse an inclined sand pile

The sandy robot should possess exceptional climbing capabilities when traversing a dune with a specific slope. Due to the loose nature of sand, the robot encounters slippage issues. Evaluating the robot's climbing ability relies on quantifying the extent of slippage through slip rate measurement. The slip rate is defined as:

$$s = \frac{v_a - v_r}{v_a} = 1 - \frac{v_r}{v_a} \tag{1}$$

where v_r is the motion velocity of the robot, v_a is the circular velocity of the origami wheel, $v_a = 2\pi r\omega$, where r is the radius of the origami wheel, and ω is the rotation speed of the wheel. The equation shows that the range of the slip rate is within the range of 0–1. For $s = 0$, forward motion of the robot does not result in wheel slippage. As the slip rate increases, the likelihood of slipping for the robot also increases. For $s = 1$, the sand robot is unable to advance because of the origami wheel slipping.

The climbing performance of the sandy robot was assessed by constructing a sand pile with the slope illustrated in Fig. 9(a). To evaluate the robot's adaptability to various slopes, dunes with angles ranging from 5° to 20° were created. The climbing capability of the robot on these slopes is depicted in Fig. 9(c). As the slope angles increase, there is an accompanying rise in slipper rate, indicating that navigating steep sand piles presents greater challenges for the robot.

The robot can adapt to sand piles with varying slopes by modifying the morphology of the origami wheel. Taking a sand pile with a slope angle of 20° as an example, we conducted tests on the climbing performance of the robot while folding the wheels into three different widths: 40, 70, and 90 mm. These three varying widths resulted in diverse climbing abilities exhibited by the robots. Notably, when unfolded to a smaller width, the robot demonstrated significantly reduced slip rates.

The origami wheels of the robot were folded to a width of 40 mm, as depicted in Fig. 9(b). Initially, within the first three seconds, the robot successfully ascended half of the slope on the dune. However, subsequently, it experienced a significant decrease in speed and began to slip and sink into the sand. Consequently, the robot started rotating in circles and formed a small depression. The wheels gradually sank deeper into the sand pile, rendering it challenging for the robot to overcome this obstacle. Conversely, when the origami wheels were unfolded to a width of 90 mm, remarkable climbing capability was exhibited by the robot. It could swiftly approach the dune and slightly decelerate while

https://doi.org/10.1017/S0263574724001619 Published online by Cambridge University Press

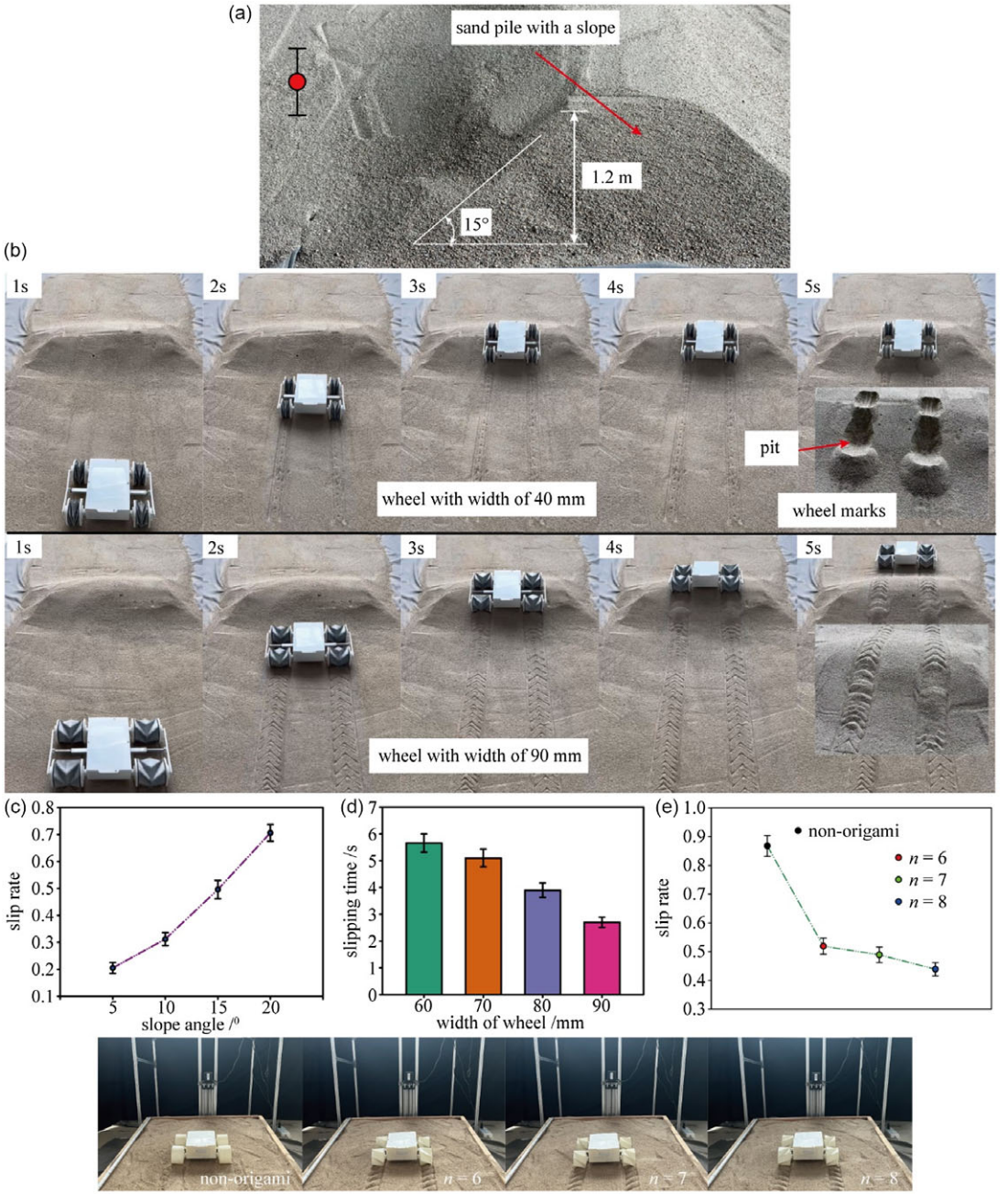

Figure 9. *Climbing performance of the sand robot. (a) The scene of a sand pile with a sloping surface. (b) The robot's locomotion on the dune with varying wheel widths. (c) The climbing capability of the robot on varying slopes. (d) The relationship between slip time and different wheel widths. (e) Comparative analysis of climbing performance between the cylindrical wheel and the origami wheel.*

ascending its slope. Throughout this process, two distinct tracks were left behind by the robot without any instances of sand depressions or pits forming. Within a span of five seconds, it effectively traversed over the dune.

https://doi.org/10.1017/S0263574724001619 Published online by Cambridge University Press

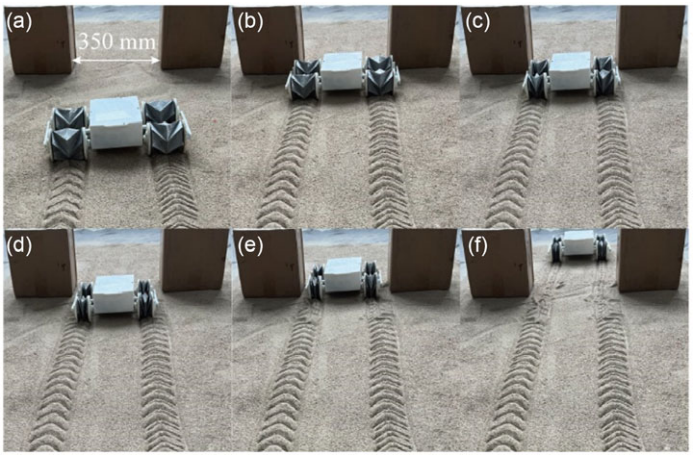

Figure 10. *Snapshots of navigating a narrow passage.*

The folding width of the origami wheels also impacts the slip time of the robot. Figure 9(d) demonstrates the relationship between slip time and different wheel widths. The experimental findings indicate that wider wheels can effectively reduce slip time, thereby increasing climbing speed.

To further demonstrate the superior adaptability of origami wheels in traversing sandy terrains, we fabricated cylindrical wheels that were similar in shape and size to origami wheels but lacked creases. We conducted a comparative analysis of climbing performance between the cylindrical wheel and the origami wheel (Fig 9e). The slip rate of the robot equipped with the cylindrical wheel reached 0.82, indicating its susceptibility to slipping. In contrast, robots equipped with origami wheels featuring 6, 7, and 8 sides maintained a consistent slip rate ranging from 0.4 to 0.5. The cylindrical wheels exhibit a smooth surface. By contrasting this smooth wheel, our intention is to demonstrate two key points: (1) the origami wheel utilizes its origami grooves, akin to thorns on a traditional wheel, to adapt effectively in sandy environments rather than solely outperforming conventional wheels; and (2) we also analyze and compare the impact of different-sided wheels on slip rates. A higher number of sides corresponds to more thorns and consequently lower slip rates, further highlighting the superior anti-slip capabilities of the origami wheel. This once again substantiates the enhanced sand climbing ability offered by origami wheels. The robot can enhance its climbing capacity on a relatively steep slope of the sand pile by adjusting the width of its wheels according to the specific sand environment it encounters.

3.5. Capacity of crossing narrow passageways

Because there are some sand piles in the sandy environment, some narrow passageways occur naturally between these sand piles. However, due to the large size and poor adaptability of traditional robots, it is difficult to cross the narrow sandy passage. Our robot can change its width to fit through this narrow passage. Figure 10 demonstrates the process of crossing the passage through the folding of the origami wheels. The width of this narrow channel is 350 mm, and the width of the robot before folding is 410 mm, so it cannot cross the channel. To adapt to this channel, we shorten the width of the robot to 300 mm by folding the origami wheel so that the robot can pass through the channel smoothly. Since the width of the wheel varies from 45 to 95 mm, the width range of the robot is [315–415] mm.

3.6. Loading capacity of the sandy robot

In addition to traversing sandy terrain, the sandy robot should possess a specific load capacity as well. When heavy objects are added to the robot, its weight increases, causing the wheels to sink into the

https://doi.org/10.1017/S0263574724001619 Published online by Cambridge University Press

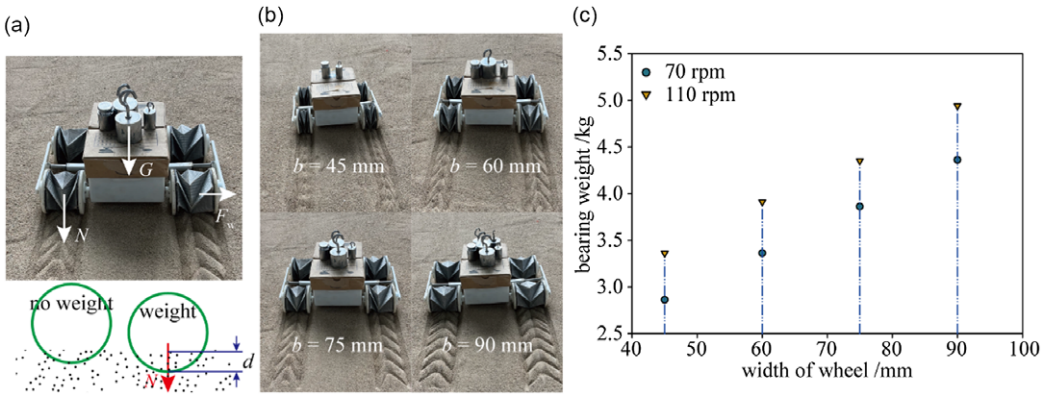

Figure 11. *Loading capacity with respect to width of the origami wheel. (a) The force exerted on the wheel by loading the weights. (b) The situation where the robot is under loads. (c) The variation of load weight corresponding to different width and rotation speed.*

sand and impeding its mobility. The load capacity refers to the ability of the robot to carry substantial loads while ensuring uninterrupted movement on sand. Due to the lightweight nature of origami wheels (with a total weight of 1.12 kg), the robot exhibits a high load bearing ratio, which represents the ratio between the carrying capacity and its own weight. Figure 11(a) illustrates various load weights when origami wheels are folded at different widths. The robot can carry weights ranging from 2.8 kg to 4.4 kg; however, expanding the origami wheels can enhance it carrying capacity further. By increasing the width of the wheels during unfolding, there is an increased contact area between each wheel and the sand surface, which reduces instances of getting stuck in sand dunes or loose soil conditions.

The increase in wheel width, as depicted in Fig. 7(d), leads to a corresponding enhancement in the robot's propulsion force, thereby strengthening robot's carrying capacity. To further illustrate this point, we conducted additional tests on the weight-bearing capability of the robot at rotation speeds of 70 and 100 rpm, respectively, with the results presented in Fig. 11(b). These findings demonstrate that augmenting the rotational speed of the wheel also enhances the robot's carrying capacity, aligning with the outcomes shown in Fig. 7(c); namely, an increased rotational speed improves both propulsion force and carrying capacity. Consequently, this results in an improved load bearing ratio ranging from 2.1 to 3.2, indicating that the robot can support two to three times its own weight.

We investigate the impact of weights on the folding behavior of origami wheels. The application of weights to the robot results in an increased overall weight, causing the wheels to sink deeper into the sand (Fig. 11a). This increased sinking depth leads to enhanced resistance (F_w) in the folding direction of the origami wheel, necessitating a higher driving force from the telescopic rod responsible for its folding. Consequently, achieving an equivalent wheel width requires greater driving force when weights are present compared to their absence.

3.7. Proof-of-concept application example

Based on the performance analysis mentioned above, our robot demonstrates its adaptability to various sandy environments by utilizing folding origami wheels. When operating in real sandy conditions, the robot will encounter situations such as narrow channels, sand slopes, and curved paths. Therefore, it is essential for the robot to be capable of performing multimodal tasks to adapt to different scenarios. To showcase this adaptability, we constructed a sand scene incorporating multiple tasks as depicted in Fig. 12. The multimodal tasks include (1) swift movement on flat sand, (2) crossing narrow channels, (3) making left turns to avoid obstacles, and (4) making right turns to avoid obstacles. To accomplish these diverse tasks effectively, it is necessary to leverage the self-folding malleability of the origami

https://doi.org/10.1017/S0263574724001619 Published online by Cambridge University Press

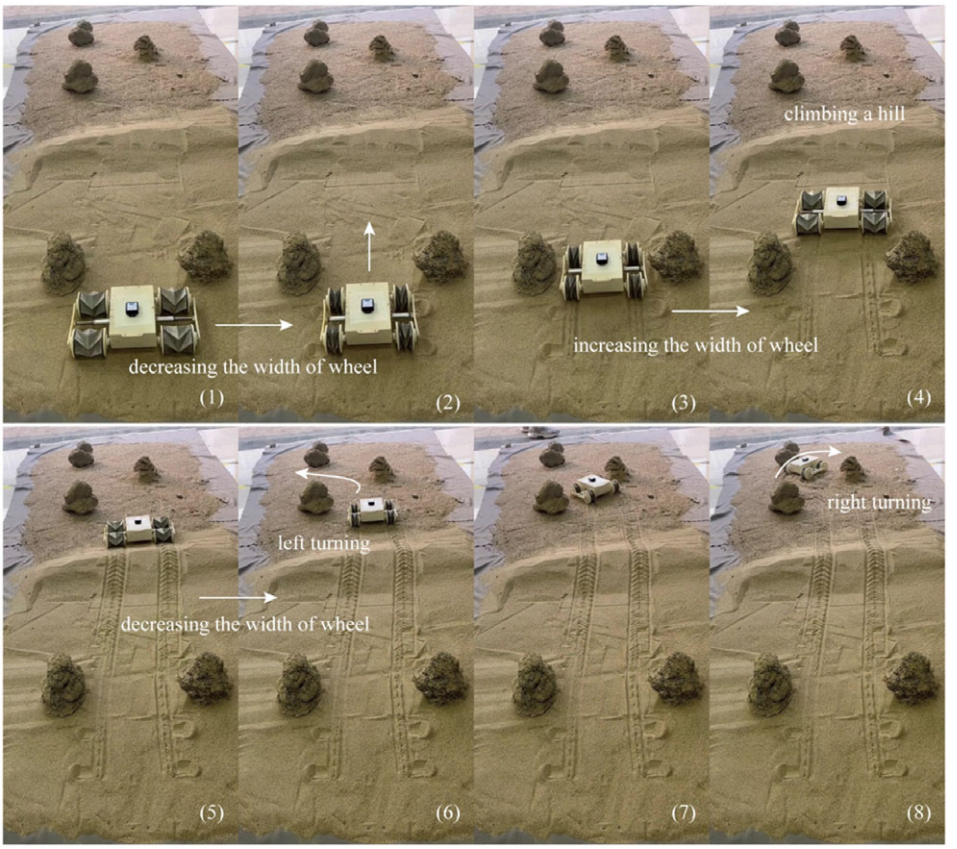

Figure 12. *Demonstration of adaptability to various sandy environments by utilizing folding origami wheels.*

wheel. First, folding the origami wheels into a larger width enhances velocity when moving across flat sand surfaces. Second, reducing their width allows smooth passage through narrow channels. Third, increasing wheel width aids climbing sandy slopes after crossing narrow passages by minimizing slippage. Lastly, adjusting rotation speed enables turning on sand and facilitates adaptation to different bending channels. Through successfully completing these multimodal tasks, our robot showcases its ability to adapt according to varying task requirements – highlighting promising prospects for practical applications of mobile robots equipped with origami wheels.

4. Conclusions

The paper presents a sand mobile robot equipped with origami wheels that possess the ability to alter their shape and size, enabling adaptation to diverse sand terrains through the utilization of origami's folding mechanism. The dynamic morphological changes exhibited by these origami wheels empower the robot to successfully undertake challenging tasks, such as traversing varying gradients of sand piles and narrower channels, which pose significant difficulties for conventional rigid mobile robots. We conducted comprehensive evaluations on how alterations in the morphology of the origami wheels impact locomotive performance, thereby providing valuable guidelines for deploying this robot in sandy environments. Experimental tests were performed to elucidate how variations in wheel width influence mobility velocity, propulsive force, climbing capability, and carrying capacity of the robot. Leveraging its folding malleability, the origami wheel facilitates efficient movement across flat sand surfaces while

https://doi.org/10.1017/S0263574724001619 Published online by Cambridge University Press

seamlessly navigating narrow channels and intelligently avoiding obstacles. In a word, our robot exhibits promising potential for practical applications.

Despite the robust adaptability of our robot in sandy environments, we have also recognized certain limitations in its research. First, further understanding is required to establish a mechanical model that accurately depicts the interaction between the origami wheel and sand. The mechanics of wheel–sand interaction are crucial for comprehending aspects such as design, performance evaluation, and control of mobile robots. Second, additional clarification is needed regarding how the polymorphism of the origami wheels affects reducing sliding subsidence caused by sand flow. Lastly, although our robot is untethered, it faces challenges in terms of long endurance due to carrying battery power; however, this challenge could potentially be overcome through future utilization of sustainable energy sources like solar power.

Financial support. The research described in this paper was financially supported by the National Natural Science Foundation of China (grant numbers 52165011), Ganzhou City Science and Technology Plan Project (2023PGX16964), the Jiangxi Natural Science Foundation of Jiangxi Province (grant number 20212BAB204028), the Key Project of Jiangxi Natural Science Foundation of Jiangxi Province (grant number 20202ACBL204009), and the Qingjiang Excellent Young Talents Program at Jiangxi University of Science and Technology (grant number JXUSTQJBJ2018006).

Competing interests. The authors declare no competing interest exist.

Author contributions. Hu Junfeng assumes a guiding role, overseeing the writing, research, and proofreading processes while also conducting an impartial review of the paper. Shu Shen and Han Weitao conceive and execute the study design as well as perform data analysis. Han Weitao is responsible for data collection, whereas Shu Shen focuses on test analysis and statistical data processing to ensure precise and high-quality results. The accuracy and validity of the data are further confirmed by Shu Shen. Additionally, due to Han's completion of the studies, Shu Shen undertakes the entire subsequent review process and carries out necessary revisions to validate the scientific integrity of this article.

References

[1] G. Ishigami, A. Miwa, K. Nagatani and K. Yoshida, "Terramechanics-based model for steering maneuver of planetary exploration rovers on loose soil," *J. Field. Robot.* **24**(3), 233–250 (2007).
[2] M. Sutoh, Y. Iijima, Y. Sakakieda and S. Wakabayashi, "Motion modeling and localization of skid-steering wheeled rover on loose terrain," *IEEE Robot. Autom. Lett.* **3**(4), 4031–4037 (2018).
[3] L. Xu, S. Zhang, N. Jiang and R. Xu, "A hybrid force model to estimate the dynamics of curved legs in granular material," *J. Terramech.* **59**(0), 59–70 (2015).
[4] T. Omura and G. Ishigami, "Wheel slip classification method for mobile robot in sandy terrain using in-wheel sensor," *J. Robot. Mechatron.* **29**(5), 902–910 (2017).
[5] J. Wang and X. Kong, "A reconfigurable tri-prism mobile robot with eight modes," *Robotica* **36**(10), 1454–1476 (2018).
[6] L. Ding, H. Gao, Z. Deng, K. Nagatani and K. Yoshida, "Experimental study and analysis on driving wheels'performance for planetary exploration rovers moving in deformable soil," *J. Terramech.* **48**(1), 27–45 (2010).
[7] H. Shibly, K. Iagnemma and S. Dubowsky, "An equivalent soil mechanics formulation for rigid wheels in deformable terrain, with application to planetary exploration rovers," *J. Terramech.* **42**(1), 1–13 (2005).
[8] H. Marvi, C. Gong, N. Gravish, H. Astley, M. Travers, R. L. Hatton, J. R. Mendelson III, H. Choset, D. L. Hu and D. I. Goldman, "Sidewinding with minimal slip: Snake and robot ascent of sandy slopes," *Science* **346**(6206), 224–229 (2014).
[9] T. Sun, X. Xiang, W. Su, H. Wu and Y. Song, "A transformable wheel-legged mobile robot: Design, analysis and experiment," *Robot. Auton. Syst.* **98**(C), 30–41 (2017).
[10] A. Ibrahim, S. Aoshima, N. Shiroma and Y. Fukuoka, "The effect of assistive anchor-like grousers on wheeled rover performance over unconsolidated sandy dune inclines," *Sensors* **16**(9), 1507–1530 (2016).
[11] C. Li, P. B. Umbanhowar, H. Komsuoglu, D. E. Koditschek and D. I. Goldman, "Sensitive dependence of the motion of a legged robot on granular media," *PNAS* **106**(9), 3029–3034 (2009).
[12] Q. Ze, S. Wu and J. Dai, "Spinning-enabled wireless amphibious origami millirobot," *Nat. Commun.* **13**(1), 1–9 (2022).
[13] D.-Y. Lee, S.-R. Kim, J.-S. Kim, J.-J. Park and K.-J. Cho, "Origami wheel transformer: A variable-diameter wheel drive robot using an origami structure," *Soft Robot.* **4**(2), 163–180 (2017).
[14] D.-Y. Lee, J.-K. Kim, C.-Y. Sohn, J.-M. Heo and K.-J. Cho, "High-load capacity origami transformable wheel," *Sci. Robot.* **6**(53), eabe0201 (2021).
[15] C. H. Belke and J. Paik, "Mori: A modular origami robot," *IEEE/ASME Trans. Mechatron.* **22**(5), 2153–2164 (2017).
[16] C. Cao, D. Moon, C. Creager, D. K. Lieu and H. S. Stuart, "Push-pull locomotion: Increasing travel velocity in loose regolith via induced wheel slip,"*J. Terramech.* **110**, 87–99 (2023).

[17] Z. Zhai, Y. Wang and H. Jiang, "Origami-inspired, on-demand deployable and collapsible mechanical metamaterials with tunable stiffness," *PNAS* **115**(9), 2032–2037 (2018).
[18] H. Zhang, "Mechanics analysis of functional origamis applicable in biomedical robots," *IEEE/ASME Trans. Mechatron.* **27**(5), 2589–2599 (2022).
[19] Y. Zhao, Y. Chi, Y. Hong, Y. Li, S. Yang and J. Yin, "Twisting for soft intelligent autonomous robot in unstructured environments," *PNAS* **119**(22), e2200265119 (2022).
[20] L. Ding, H. Gao, Z. Deng and J. Tao, "Wheel slipsinkage and its prediction model of lunar rover," *J. Central South Univ. Technol.* **17**(1), 129–135 (2010).
[21] C. Ai, Y. Chen, L. Xu, H. Li, C. Liu, F. Shang, Q. Xia and S. Zhang, "Current development on Origami/Kirigami-inspired structure of creased patterns toward robotics," *Adv. Eng. Mater.* **23**(10), 2100473 (2021).
[22] Y. S. Kim, G. P. Jung, H. Kim, K. J. Cho and C. N. Chu, "Wheel transformer: A wheel-leg hybrid robot with passive transformable wheels," *IEEE T. Robot.* **30**(6), 1487–1498 (2014).
[23] L. Chang, J. W. Samuel, B. Maria, P. Taskin and M. Samuel, "Shake and take: Fast transformation of origami gripper," *IEEE Trans. Robot.* **38**(1), 491–506 (2022).

Cite this article: J. Hu, S. Shu and W. Han (2024). "A novel mobile robot with origami wheels designed for navigating sandy terrains", Robotica **42**, 3731–3747. https://doi.org/10.1017/S0263574724001619